BNL–45521
AD/RHIC–96
Conference Paper

Correction of Skew-Quadrupole Errors in RHIC

G. F. Dell, H. Hahn, S. Y. Lee, G. Parzen and S. Tepikian

May 1991

R H I C P R O J E C T

Brookhaven National Laboratory
Associated Universities, Inc.
Upton, NY 11973

Under Contract No. DE–AC02–76CH00016 with the
UNITED STATES DEPARTMENT OF ENERGY

1991 IEEE Particle Accelerator Conference
San Francisco, CA
May 6-9, 1991

BNL-45521

CORRECTION OF SKEW–QUADRUPOLE ERRORS IN RHIC*

G.F. Dell, H. Hahn, S.Y. Lee†, G. Parzen and S. Tepikian

Brookhaven National Laboratory
Upton, NY 11973, USA

Abstract

The correction scheme for skew–quadrupole (a_1) errors in the Relativistic Heavy Ion Collider is presented. The a_1 errors result from fabrication and from installation errors. At the selected betatron tune of $\nu_x = 28.826$ and $\nu_y = 28.820$, the principal resonances driven by a_1 errors are $\nu_x - \nu_y = 0$, the sum resonances near $\nu_x + \nu_y$ which cause residual tune splitting and distortion of beta function, and $\nu_y = 28\&29$ which cause vertical dispersion. Skew quadrupole correctors located in the insertions and arcs will be used to correct the coupling and sum resonances and, if required, separate correctors in the arcs could be used for vertical dispersion correction. The study of the a_1 correction system confirmed that correction is possible at $\beta^* = 2$ m and $\beta^* = 6$ m and that the required corrector strengths are consistent with those specified for RHIC.

INTRODUCTION

The correction system for the skew–quadrupole errors in RHIC, the Relativistic Heavy Ion Collider, is discussed in this paper. The most important effect of these errors is the tune splitting associated with the $\nu_x - \nu_y = 0$ coupling resonance. This effect can be corrected to a large degree with a two–family corrector system that corrects the driving term of the resonance.[1] Two other effects induced by skew–quadrupoles are residual tune splitting that remains after the driving term of the $\nu_x - \nu_y = 0$ resonance has been corrected and distortion of the beta functions.[2–3] These two effects have been found to be associated with the sum resonances near $\nu_x + \nu_y$.[2-4] Skew–quadrupoles also produce vertical dispersion that is associated with the integer resonances at $\nu_y = 28\&29$.

A system of skew correctors will be provided in RHIC to counteract the beam dynamic effects mentioned. The correctors are located in the insertions as well as arcs. Several configurations were investigated and served as a guide in selecting the present version in which the number of cold–to–warm feedthroughs and the number of power supplies required at start–up was minimized.[5,6] In fact, only correction of the coupling resonance will initially be available.

The performance of the skew–quadrupole correction system is evaluated by determining its ability to correct the important stopbands of the resonances associated with the four effects mentioned above. The capacity and flexibility of the system will be demonstrated by correcting the $\nu_x - \nu_y = 0$ and the $\nu_x + \nu_y = 58\&59$ stopbands. However, the system is sufficiently flexible to be operated in ways which correct the beam dynamic effects directly without reference to stopbands.

SKEW–QUADRUPOLE ERRORS

The a_1 errors consist of construction errors from coil tolerances in the dipoles resulting in $a_1 \approx 1.7 \times 10^{-4}$ cm^{-1} rms as well as errors from an anticipated 0.5 mrad rms uncertainty in the orientation of the planes of the quadrupoles that is a combination of field measurement errors and installation errors. Furthermore, solenoids which are part of experimental detectors at the crossing points will be a skew–quadrupole source.

The complex strength of the stopband integrals and driving terms can be approximated by the sums listed in Table I. Estimates of their strength were made with random a_1 errors generated according to a Gaussian distribution that is truncated at $\pm 3\sigma$. A systematic error was added to the arc dipole errors to produce a 0.3σ average a_1. The maximum expected stopband/driving terms were estimated by sampling 10 machines with the results given in Table II.

Sorting of arc dipoles can be used to reduce the driving terms. It is planned to sort in a way which reduces vertical dispersion resulting in an error reduction by a factor of 2-3. It is expected that sorting eliminates the need for vertical dispersion correction, nevertheless the capability will be provided.

Table I: Stopband Integrals and Driving Terms.

$$\Delta_0 = \frac{1}{4\pi}\sum \frac{a_1 \ell}{\rho}\sqrt{\beta_x\beta_y}\exp i\,(\varphi_x - \varphi_y)$$

$$\Delta_{57} = \frac{1}{4\pi}\sum \frac{a_1 \ell}{\rho}\sqrt{\beta_x\beta_y}\exp i\left(\frac{28.5}{\nu_x}\varphi_x + \frac{28.5}{\nu_y}\varphi_y\right)$$

$$\Delta_{58} = \frac{1}{4\pi}\sum \frac{a_1 \ell}{\rho}\sqrt{\beta_x\beta_y}\exp i\left(\frac{29}{\nu_x}\varphi_x + \frac{29}{\nu_y}\varphi_y\right)$$

$$\Delta_{28} = \frac{\nu_y}{4\pi}\sum \frac{a_1 \ell}{\rho}X_p\sqrt{\beta_y}\exp i\left(\frac{28}{\nu_y}\varphi_y\right)$$

$$\Delta_{29} = \frac{\nu_y}{4\pi}\sum \frac{a_1 \ell}{\rho}X_p\sqrt{\beta_y}\exp i\left(\frac{29}{\nu_y}\varphi_y\right)$$

*Work performed under the auspices of the U.S. Department of Energy.

†Present address: Dept. of Physics, Indiana University, Bloomington, IN 47405.

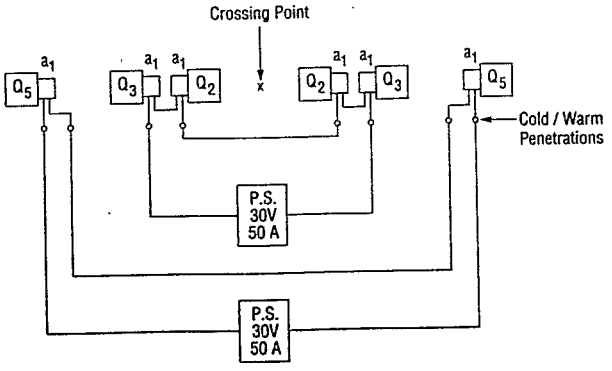

Fig. 1: Insertion corrector configuration.

CORRECTOR SYSTEM

The RHIC lattice consists of three superperiods each having an inner arc of 12 cells, an In–Out insertion, an outer arc of 12 cells, and an Out–In insertion. The insertions are identified by their location on the face of the clock as 2:, 6:, 10: and 4:, 8:, 12:, respectively. The phase advance per cell is approximately 90°. The location of the a_1 correctors in the insertions is shown in Fig. 1 and of the arc correctors in Fig. 2. The standard–aperture correctors, i.e. in the arcs and in the insertion at Q5, have a strength of 1.5 T. The large–aperture correctors are weaker, but the combination of one corrector each at Q2&Q3 also provide 1.5 T.

The correction scheme adopted assumes families of correctors, representing a group of correctors with separate power supplies, which are software coupled. Considerable effort went into finding families which are orthogonal due to their hardware configuration.

Table II: Estimates of Correction Requirements: Stopband/Driving Term Strengths.

	$\beta^* = 2$ m		$\beta^* = 6$ m		
	Re	Im	Re	Im	Units
"0"	7.6	4.4	7.2	1.0	$\times 10^{-2}$
"57"	3.1	4.8	2.2	2.6	$\times 10^{-2}$
"58"	3.6	2.0	2.3	1.7	$\times 10^{-2}$
"28"	17.8	8.5	17.8	9.4	$\times 10^{-2}$ m$^{1/2}$
"29"	9.6	13.6	8.9	13.6	$\times 10^{-2}$ m$^{1/2}$

The two families required for correction of linear coupling are obtained in the case of:

$\beta^* = 2$ m with (Q3 @ 2: 6: 10: + Q3 @ 4: 8: 12:) and (Q3 @ 2: 6: 10: − Q3 @ 4: 8: 12:) producing real and imaginary terms respectively;

$\beta^* = 6$ m with (Q3 @ 2: 6: 10: + Q3 @ 4: 8: 12:) and (Q5 @ 2: 6: 10: − Q5 @ 4: 8: 12:). On day–one only the linear–coupling correction system will be powered.

The two families for correction of the "57" stopband involve the 3×8 correctors each in the outer arcs (QO) and in the inner arcs (QI). Within one arc there are 4 positive and 4 negative correctors cancelling a contribution to "0". (However, the wiring maintains the option of locally correcting an average a_1 in the arc.)

The correction scheme for "58" takes advantage of the 120° phase shift between superperiods which leads to $1 - \frac{1}{2}e^{i120} - \frac{1}{2}e^{-i120} = 0$ assuring orthogonality with "0" and "57". The two families are then (Q3 @ 2: $-\frac{1}{2}$6: $-\frac{1}{2}$10:) and (Q3 @ 4: $-\frac{1}{2}$8: $-\frac{1}{2}$12:).

The remaining 12 independent corrector pairs in the arcs will be available for vertical dispersion correction. Each pair is counterphased and thus orthogonal to "0". These correctors could be combined into four families to correct "28" and "29" or alternatively to correct directly the vertical dispersion at the crossing points.

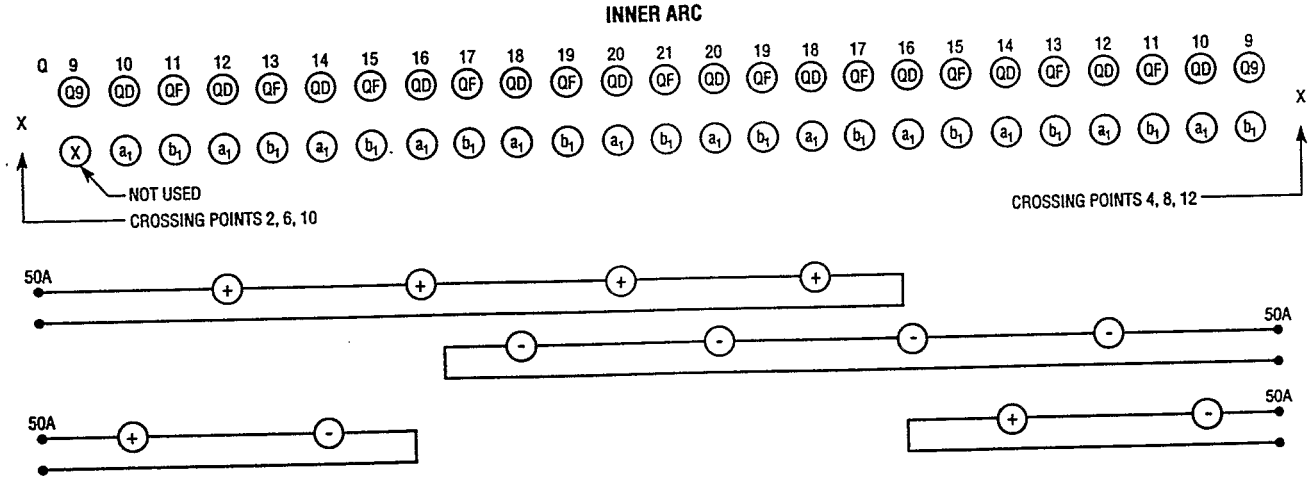

Fig. 2: Arc corrector configuration.

Table III: Stopband Matrix (Δ in units of 10^{-2}).

$$\begin{pmatrix} \mathrm{Re0} \\ \mathrm{Im0} \\ \mathrm{Re57} \\ \mathrm{Im57} \\ \mathrm{Re58} \\ \mathrm{Im58} \end{pmatrix} = \begin{pmatrix} 33.1 & 1.1 & 0 & 0 & 0 & 0 \\ 0.7 & -54.9 & 0 & 0 & 0 & 0 \\ 1.8 & 32.6 & -5.9 & -3.6 & 0 & 0 \\ -1.1 & 54.7 & 3.9 & -6.0 & 0 & 0 \\ 0 & 0 & 0 & 0 & -4.3 & 15.7 \\ 0 & 0 & 0 & 0 & 15.4 & -3.0 \end{pmatrix} \begin{pmatrix} \mathrm{Q3}\,(2{:}\,6{:}\,10{:}\,{+}4{:}\,8{:}\,12{:}) \\ \mathrm{Q3}\,(2{:}\,6{:}\,10{:}\,{-}4{:}\,8{:}\,12{:}) \\ \mathrm{QO} \\ \mathrm{QI} \\ \mathrm{Q3}\,(2{:}\,{-}\tfrac{1}{2}6{:}\,{-}\tfrac{1}{2}10{:}) \\ \mathrm{Q3}\,(4{:}\,{-}\tfrac{1}{2}8{:}\,{-}\tfrac{1}{2}12{:}) \end{pmatrix}$$

STOPBAND MATRIX AND CAPABILITIES

The impact of each corrector family on all stopbands can be represented in matrix form which indicates the real and imaginary stopband produced by full–strength excitation of the correctors in a family. For example, the matrix for $\beta^* = 2$ m in all insertions is shown in Table III.

The correction capability for each stopband was obtained by inverting a related matrix which connects the individual corrector to the stopbands, and by determining the maximum modulus $|\Delta|$ that can be achieved with 1.5 T corrector strength. In cases where one corrector is required for two stopbands, a strength of 1.5 T/$\sqrt{2}$ was allotted to each stopband. The resulting correction capabilities for $\beta^* = 2$ m are shown in Fig. 3 and are compared to the error estimates. The capability of the system would seem sufficient to correct the skew–quadrupole errors with a 95% confidence level. The correction requirements for $\beta^* = 6$ m are less stringent.

SIMULATION RESULTS

The operation of the a_1 correction system was simulated using the *PATRICIA* tracking program for ten sets of random errors. The "0", "57" and "58" stopband integrals were evaluated and used to obtain the required corrector strength. With the correctors powered, the stopbands were reduced by a factor of 10^3.

In order to study tune splitting, the tune was set to $\nu_x = 28.826$ and $\nu_y = 28.820$ when skew–quadrupoles are absent. Introduction of skew–quadrupole errors produces tune splitting, $\nu_1 - \nu_2$. The tunes, before and after stopband correction, were obtained by Fourier analysis of 2000 turn tracking runs. The rms tune splitting was determined for the 10 sets of random errors to be $\Delta\nu \approx 124 \times 10^{-3}$ rms for $\beta^* = 2$ m and 110×10^{-3} rms for $\beta^* = 6$ m. Correction of the "0" stopband reduced the tune splitting by more than one order of magnitude.

In conclusion, the simulation studies confirmed that the a_1 correction system has the strength and flexibility to cope with the expected skew–quadrupole errors.

REFERENCES

[1] G. Parzen, BNL Report AD/RHIC–AP–72, (1988).

[2] G. Parzen, BNL Report AD/RHIC–82 (1990).

[3] G. Parzen, BNL Report AD/RHIC–73 (1990).

[4] G. Parzen, *Tune splitting in the presence of linear coupling*, (these proceedings).
G. Parzen, *Beta functions in the presence of linear coupling*, (these proceedings).

[5] H. Hahn and G. Parzen, BNL Report AD/RHIC–RD–20 (1990).

[6] S.Y. Lee and S. Tepikian, BNL Report AD/RHIC–75 (1990).

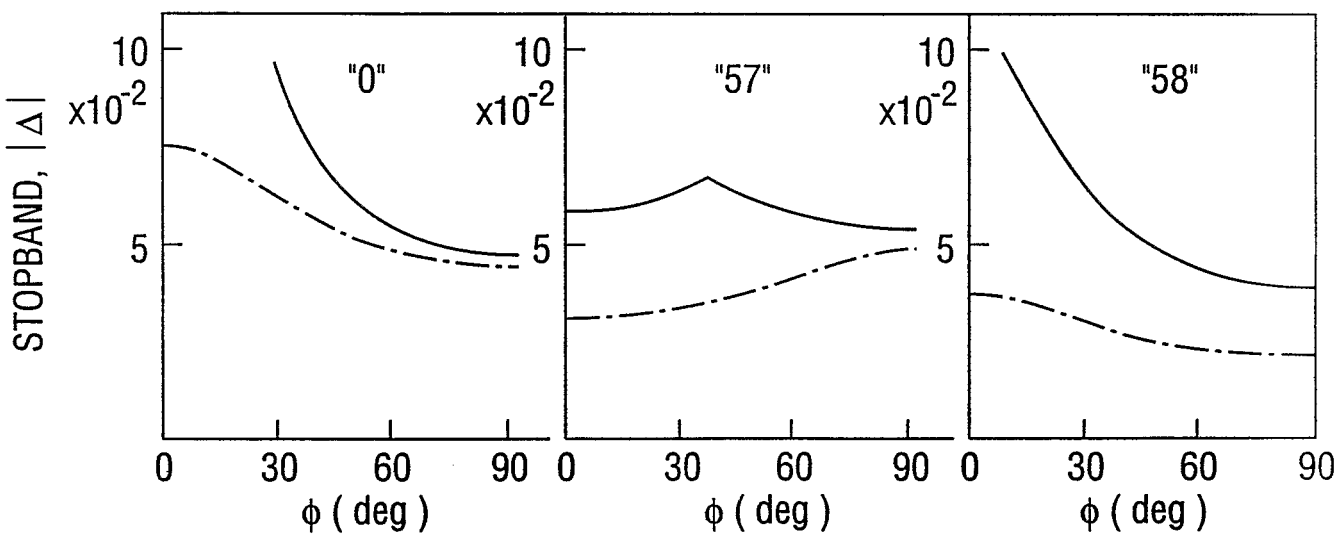

Fig. 3: Stopband corrector capability (solid line) and requirements (dashed lines) for $\beta^* = 2$ m.